

CHEMISTRY & SUSTAINABILITY

CHEM **SUS** CHEM

ENERGY & MATERIALS

Accepted Article

Title: Operando Catalysis Reveals the Superior Cracking Activity and Stability of Hierarchical ZSM-5 for the Cracking of LDPE

Authors: Karolina Tarach, Kamila Pyra, Sandra Siles, Ignacio Malian-Cabrera, and Kinga Góra-Marek

This manuscript has been accepted after peer review and appears as an Accepted Article online prior to editing, proofing, and formal publication of the final Version of Record (VoR). This work is currently citable by using the Digital Object Identifier (DOI) given below. The VoR will be published online in Early View as soon as possible and may be different to this Accepted Article as a result of editing. Readers should obtain the VoR from the journal website shown below when it is published to ensure accuracy of information. The authors are responsible for the content of this Accepted Article.

To be cited as: *ChemSusChem* 10.1002/cssc.201802190

Link to VoR: <http://dx.doi.org/10.1002/cssc.201802190>

WILEY-VCH

www.chemsuschem.org

A Journal of



Operando Catalysis Reveals the Superior Cracking Activity and Stability of Hierarchical ZSM-5 for the Cracking of LDPE

Karolina A. Tarach,^[a] Kamila Pyra,^[a] Sandra Siles,^[b] Ignacio Melián-Cabrera,^[b] Kinga Góra-Marek^{[a]*}

Abstract: In this communication, a new theoretical and practical framework through Operando Catalysis to study the zeolite catalytic cracking of the low-density polyethylene as model reaction, under reaction conditions is provided. Results show that a microporous ZSM-5 gives rise to less cracking products. Hierarchical ZSM-5 zeolites are more cracking active, rendering more C₂-C₅ hydrocarbons, with a delayed deactivation due to the secondary porosity. This tool in combination with thermogravimetric analysis provides complementary and valuable information for the study, and design of advanced catalysts.

For many years, there has been a continuous increase in the number of plastic products, without control in their management after use. Therefore, the use of plastic is often associated with plastic waste and a common way to dispose of it is landfilling. Considering that polyethylenes (PEs) are characterized by a slow degradation rate, and a threat to the environment, the current plastic waste is a well-recognized environmental problem. For this reason, it is imperative to develop new methods of PEs waste handling.^[1] Thermal cracking is known as the simplest process for recycling waste plastic; it consists of the rapid heating in the absence of oxidant. As a result, hydrocarbons with a wide range of molecular weights are obtained. The relatively high temperature necessary for polymer cracking, product quality and, therefore the overall efficiency, are the main drawbacks. State-of-the-art methods for waste plastic include catalytic pyrolysis using zeolites as advanced materials.^[1c, 2] Different catalysts have been investigated in the catalytic pyrolysis of plastics, allowing to lower the process temperature and improve the selectivity of more-desired products. Zeolites (ZSM-5, USY) have provided attractive results, associated with their acidic properties and porous structure.^{[1a], [3]} The acid sites, in particular, their strength and distribution are key parameters affecting the rate and selectivity.^[1a, 1b, 2a, 2c, 3c, 4] It is assumed that the first step of the catalytic cracking of hydrocarbons is the activation of olefin or paraffin on the acid sites proceeding with the formation of organic carbocations, in particular, carbenium and carbonium ions.^[5] The use of these acid catalysts is reflected in the appearance of C₂-C₄

olefins, and usually, the higher the strength of the acid sites, the more effective is the cracking of the polymer chains.^[2a, 6] Seo *et al.* reported that the ZSM-5, USY and mordenite zeolites in the HDPE pyrolysis at 450°C, gave high yields of valuable gases, with 64% for ZSM-5 as the optimal. The high ZSM-5 efficiency was ascribed to the high site acid strength and microporous structure, exhibiting excellent effectiveness in cracking, isomerisation and aromatization.^[7] The activity and selectivity of zeolites depend on many factors, of which acidity is the most important, due to the role of acid sites in the degradation mechanism.^[8] Despite these promising results, microporous ZSM-5 often has limitations in the molecular transport of reagents, especially in polymer cracking reactions involving bulky molecules. In addition, the long diffusion pathways of molecules in the zeolite micropores lead to the formation of coke, therefore deactivating the catalyst. The introduction of secondary porosity to microporous ZSM-5, also known as mesoporous- or hierarchical zeolites, results in the shortening of the diffusion path and this increases the acid site accessibility, whereas coking is limited.^[1b, 9]

The PEs catalytic process is typically evaluated by thermogravimetric or a batch reactor, where either weight or reaction liquids are analysed on time. One of the areas that have been hardly investigated in this application is the operando catalysis, *i.e.* using a reactor where the catalyst is monitored during the reaction. Such an approach can provide crucial information about the cracking reactions on the catalyst surface as well as about the deactivation process under the working conditions. To the best of our knowledge, this approach has not been reported in the waste plastic cracking catalysis.

Here, it is shown that such an approach renders unprecedented

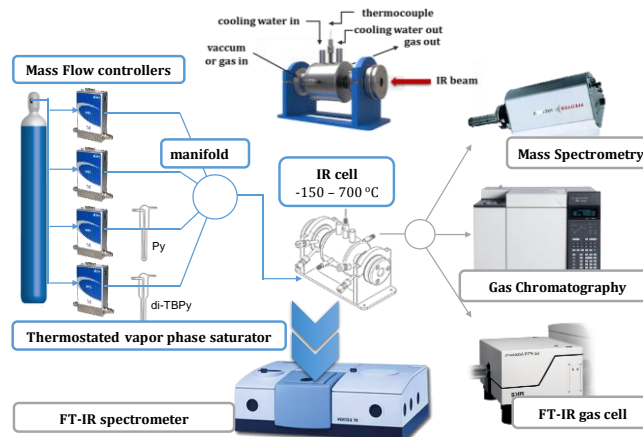


Figure 1. On-purpose designed operando IR cell embedded in a flow system, with four detections systems: IR MCT detector, mass spectrometry, gas chromatograph and IR gas cell.

[a] Dr. Karolina A. Tarach, MSc Kamila Pyra, Prof. Kinga Góra-Marek
Faculty of Chemistry, Jagiellonian University in Kraków, 2
Gronostajowa St., 30-387 Kraków, Poland
** E-mail: kinga.gora-marek@uj.edu.pl

[b] MEng. Sandra Siles, Dr. Ignacio Melián-Cabrera
European Bioenergy Research Institute, School of Engineering and
Applied Science, Aston University, Birmingham B4 7ET,
United Kingdom.

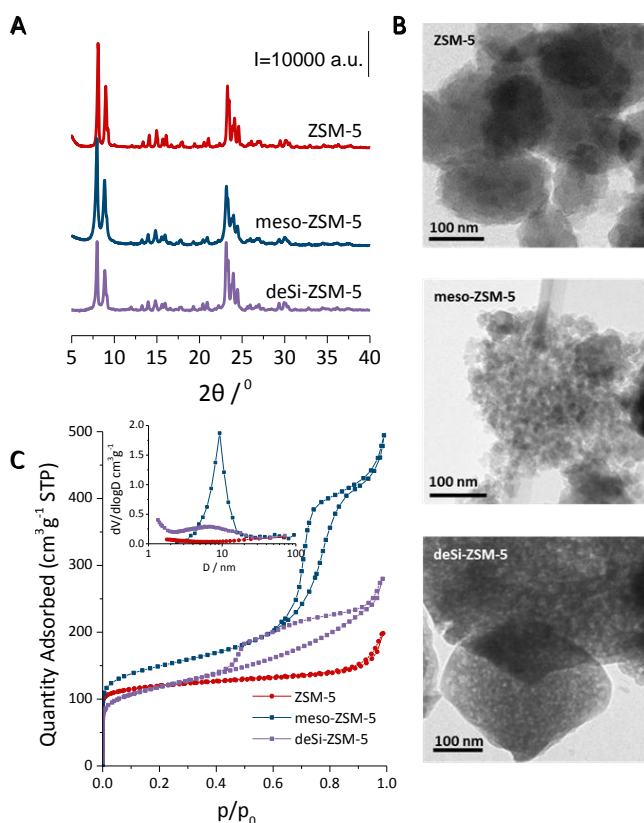


Figure 2. A) XRD patterns, B) TEM micrographs and C) N_2 adsorption-desorption isotherms and BJH pore size distributions (inset).

information that allows to design new, more advanced, catalysts. On this basis, an on-purpose built operando reactor was designed (Figure 1). It consists of a feeding system, where probe molecules through saturators, or reactive/inert gases, can be fed through the catalyst. The gas/vapour goes through a tailor-made IR cell, where the polymer/catalyst wafer is placed. The catalyst surface is monitored by rapid-scan IR whereas the gaseous products are analysed by gas chromatography and mass spectroscopy.

The study is illustrated with ZSM-5 zeolite as a case study. Several types were prepared; one mainly displaying micropores and two cases having mesoporosity of increasing degree. Characterisation of the materials were carried out comparatively. Elemental analysis by ICP (Table 1) reveals that the Si/Al ratio is comparable, in the range of 23 to 30. XRD patterns (Fig. 2A) reveal that the MFI structure is present in all the materials. The crystallinity of the deSi-ZSM-5 is reduced due to the massive presence of mesopores. This is evident in the TEM (Fig. 2B) where this material displays gruyere-cheese intraparticle mesopores, extended widely across the crystals. ZSM-5 does not display any appreciable intra-crystalline porosity, while the meso-ZSM-5 is characterised by an agglomerate of ZSM-5 particles with high inter-particulate pores. These results are confirmed by N_2

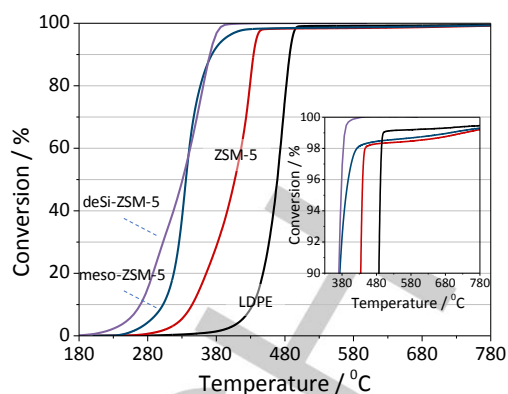


Figure 3. Conversion curves of LDPE cracking over the studied zeolites, including the thermal cracking.

adsorption measurements (Fig. 2c) where the mesoporosity is well seen for meso-ZSM-5 and desi-ZSM-5. In the case of the desi-ZSM-5, a closure point at $p/p_0 \sim 0.42$ indicates the possibility to have restricted smaller pores because the TSE effect masks smaller restrictions.^[11] This effect is absent in the meso-ZSM-5 where the closure point is located at ~ 0.60 . Therefore, this hierarchical zeolite is more accessible than the desi-ZSM-5. The textural parameter (S_{meso}) varies in that direction with 44, 187 and 214 m^2/g , while the micro-porosity changes in the opposite way (cf. V_{micro}), Table 1. Therefore, these zeolites represent well-described ZSM-5 structures with different porosity. Acidity evaluation with pyridine gives an estimate of the overall acid sites since pyridine is accessible into the ZSM-5 micropores with values ranging 449 to 653 $\mu\text{mol/g}$ which agrees with the Al measured by ICP (Table 1). Therefore, Al present in these materials is quite accessible, or in other words, the amount of clustered AlO_x is small. The accessible Al was quantified with 2,6-di-tert-butylpyridine as a probe molecule; this allows to define the accessibility factor ($\text{AF}_{\text{di-TBPY}}$) as the ratio between the sites detected by di-TBPY and the ones detected by pyridine (Table 1). In line with the porosity, and shape of the isotherms, the $\text{AF}_{\text{di-TBPY}}$ for the ZSM-5 was of 6%. This increased to 27% for desi-ZSM-5 and was the highest for meso-ZSM-5 with 38%. The strength of the sites was determined by CO adsorption, in the shift of the OH band upon CO adsorption ($\Delta\nu_{\text{CO}\dots\text{OH}}$). This parameter is considered to represent well the strength of the acid sites.^[12] The shift was highest for the ZSM-5 with 316 cm^{-1} , but it did not change significantly for the hierarchical zeolites with 311 and 312 cm^{-1} .

This characterisation shows that the zeolites represent well a ZSM-5 with comparable acid strength whilst the accessibility varies among them. These modifications will have an impact in the cracking of the LDPE. Figure 3 shows the conversion curves of the various ZSM-5 catalysts as well as the thermal decomposition. The zeolites are able to decrease the reaction temperature, as it is commonly expected. The microporous ZSM-5 is however giving a limited reduction of the cracking temperature due to the limited external surface area and

Table 1. Chemical composition and textural properties derived from N_2 physisorption of and micro/mesoporous zeolites, the amounts of Al derived from ICP analysis, concentration of Brønsted (C_B) and Lewis (C_L) acid sites, the acid strength of Si-OH-Al groups ($\Delta\nu_{\text{OH}\dots\text{CO}}$) and accessibility of sites expressed as concentration of sites reached by di-TBPY and accessibility factor - $\text{AF}_{\text{di-TBPY}}$.

	Si/Al ^a	Al ^a	S_{BET} ^b	V_{micro} ^c	V_{meso} ^d	S_{meso} ^e	C_B	C_L	$C_B + C_L$	$C_{\text{di-TBPY}}$	$\text{AF}_{\text{di-TBPY}}$	$\Delta\nu_{\text{CO}\dots\text{OH}}$
		[$\mu\text{mol}\cdot\text{g}^{-1}$]	[$\text{m}^2\cdot\text{g}^{-1}$]	[$\text{cm}^3\cdot\text{g}^{-1}$]	[$\text{cm}^3\cdot\text{g}^{-1}$]	[$\text{m}^2\cdot\text{g}^{-1}$]			[$\mu\text{mol}\cdot\text{g}^{-1}$]		[%]	[cm^{-1}]
ZSM-5	30	502	459	0.17	0.06	44	386	75	461	24	6	316
meso-ZSM-5	29	518	520	0.16	0.35	187	342	107	449	139	38	312
deSi-ZSM-5	23	656	422	0.11	0.37	214	476	177	653	130	27	311

a. concentration of Al obtained from chemical analysis (ICP); b. calculated via BET method with the recommendations of Rouquerol *et al.*^[10]; c. calculated using the t -plot method; d. calculated via the BJH model using the adsorption branch.

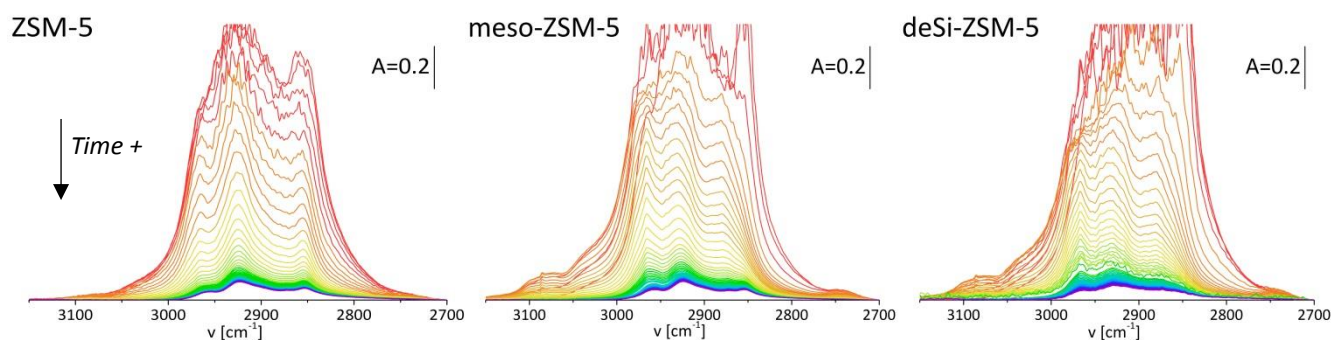


Figure 4. Rapid-scan operando FT-IR spectra of C-H stretching region during the LDPE cracking at 230 °C, the species present on the catalyst surface.

accessibility factor as discussed before. In the case of the hierarchical zeolites, both meso-ZSM-5 and deSi-ZSM-5, reduces notably the cracking temperature. The quantification of the overall reaction products by GC-MS shows that both mesoporous zeolites yield more value-added gases, C₂-C₅ with a decrease of the liquid (C₆₊), related to the higher cracking efficiency (Table 2). This phenomenon was studied by a time-resolved operando reactor of the LDPE cracking on the zeolites. The analysis was carried out from room temperature up to the total LDPE decomposition. For clarity only the IR spectra recorded at 230 °C in a function of time for the C-H stretching region are given in Figure 4. Particular effects were found when observing the -CH₃ (2960 cm⁻¹) and -CH₂ (2925 cm⁻¹) groups. The intensities of these bands were quantified and the ratio -CH₃/CH₂ was used to assess the PE end-chain cracking. The correlations were plotted in Figure 5. For the microporous ZSM-5, the ratio increases in the first 5 mins, indicating cracking over the external surface of the zeolite; however, the ratio only arrives to 0.75 and then decreases on time rapidly. This effect is attributed to: a) the deactivation (coke formation) on the external surface of the zeolite and b) the own consumption of LDPE, in other words, the reactant becomes limiting on time since the experiment is a batch type. The trend for the deSi-ZSM-5 is much more pronounced; the ratio increases much more up to 1.1 and the deactivation occurs after 10 min and is much slower than the ZSM-5. As far as the meso-ZSM-5 is concerned, the effect is the most pronounced in the cracking of the PE branches with a slower deactivation. The higher ratio (~1.25) implies a higher fraction of non-condensable gases in the product (C₃-C₅) distribution, as shown by GC/MS analyses due to the more effective cracking in the open pores. (Table 2). The spent catalysts

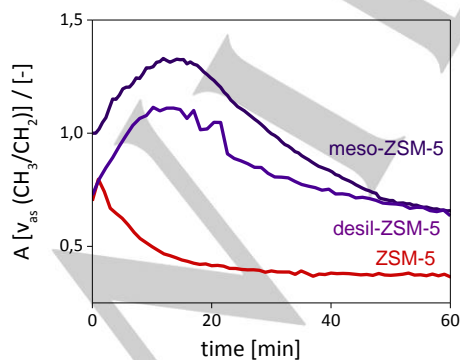


Figure 5. Operando determined [-CH₃/CH₂] ratio as a function of the reaction time for the various ZSM-5 zeolites.

were also studied by the Raman and IR spectroscopies toward an identification of carbonaceous entities with short-range order and molecular structures. The ratio between the intensity of the bands associated with the C=C stretching vibrations of conjugated olefins and the isolated C=C double bonds in disordered aromatic structures^[13] quantifies the deactivation process. The Figure 6 shows the evolution of higher amounts of carbonaceous species in the mesoporous zeolites than in micropore analogue. More open structures were also prone to arouse rapid formation of isobutane (3085 cm⁻¹, Fig. 4) and further the conjugated olefinic entities in oligomerization.

Table 2. Product distribution from the catalytic LDPE cracking.

Material	C ₃	C ₄	C ₅	C ₅₊
	[%]			
ZSM-5	13	24	21	41
meso-ZSM-5	14	28	24	34
deSi-ZSM-5	13	28	30	29

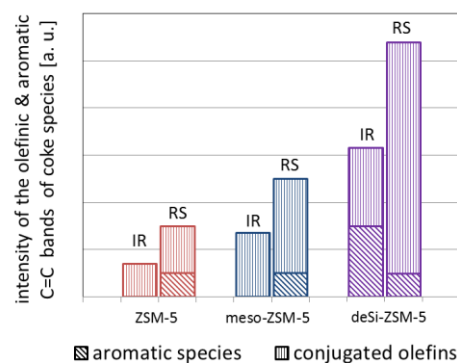


Figure 6. Speciation of carbonaceous entities for the spent zeolites ZSM-5.

Therefore, this simple technique provides a good insight on the accessibility, a qualitative indication of the non-condensable gases produced as well as the rate of deactivation; therefore, providing complementary information to the TGA, that can enable the design of more selective catalysts, if other regions of the spectra are analysed.

In conclusion, operando catalysis spectroscopy is a powerful method for the description of the speciation on surface on a working zeolite catalyst. Operando Catalysis complimented by thermogravimetric

analysis provides the evidence that the enhancement of the textural properties of mesostructured zeolites ZSM-5 is advantageous in the catalytic cracking of low-density polyethylene (LDPE) rendering more C₂-C₅ hydrocarbons, with a delayed deactivation due to the secondary porosity. The favored generation of liquid fraction (C₆₊) together with a faster deactivation is forced by the space-restricted microporous environment.

Experimental

A. Materials

A.1. Microporous ZSM-5

Microporous zeolite ZSM-5 (denoted as ZSM-5) with a Si/Al = 30 was synthesized using a gel composition of 2.0 NaCl : 1.67 Al₂O₃ : 100 SiO₂ : 20 TPA₂O (Tetrapropylammonium oxide) : 200 H₂O. In a typical synthesis, 0.69 g NaCl and 4.0 g aluminium isopropoxide were dissolved in 212 g TPAOH (tetrapropylammonium hydroxide) solution (TCl, 20-25 wt.% in H₂O). Then, 122 g TEOS (Tetraethyl Silicate) was added under vigorous stirring and the reaction mixture was stirred for 3 h at room temperature. The resultant mixture was heated at 90 °C on a hot plate under stirring to evaporate ethanol and extra H₂O to obtain the above-mentioned gel composition. The resulting gel was transferred into a Teflon-lined stainless-steel autoclave and was hydrothermally treated at 180 °C for 72 h. After cooling to room temperature, the zeolite product was filtered and washed thoroughly with deionized water. The product was dried in an oven at 130 °C and subsequently calcined in air at 600 °C for 6 h. Next fourfold Na⁺/NH₄⁺ ion-exchange steps with 0.5 M NH₄NO₃ was carried out at 60 °C for 1 h. The resulting sample was calcined at 550 °C for 2 h to provide their protonic forms.

A.2. Mesoporous ZSM-5 zeolite

Mesoporous zeolite meso-ZSM-5 (denoted as meso-ZSM-5) with Si/Al = 29, was obtained via a direct synthesis route using the amphiphilic organosilanes as a mesopore-directing agent^[14] according to the procedure described below. The TPOAC (3-(trimethoxysilyl)propyl)octadecyldimethylammonium chloride, Aldrich, 42 wt.% in methanol) was added to a conventional ZSM-5 synthesis gel containing TPABr (tetrapropylammonium bromide). In a typical synthesis, a solution consisting of 1.77 g NaOH, 2.75 g TPABr, 6.09 g TPOAC, and 130 g H₂O was prepared. Then, 21.5 g TEOS (tetraethylorthosilicate) was added and the solution was stirred for 1 h. Next, 1.72 g Al₂(SO₄)₃·18H₂O was dissolved in 37.0 g of H₂O; this was added to the aforementioned solution and finally it was homogenized by manually. The synthesis gel was stirred at room temperature for 24 h for aging. The resultant gel was hydrothermally treated in a tumbling autoclave at 170 °C for 72 h. After crystallization, the precipitated product was filtered, washed with distilled water, dried at 110 °C and calcined at 550 °C. Finally, fourfold Na⁺/NH₄⁺ ion-exchange steps with 0.5 M NH₄NO₃ were carried out at 60 °C for 1 h. The resulting sample was calcined at 550 °C for 2 h to provide the protonic form.

A.3. Desilicated ZSM-5 zeolite

The desilicated ZSM-5 (denoted as desi-ZSM-5) with Si/Al = 23 was obtained by treatment of a native ZSM-5 zeolite (Zeolyst, CBV5524G, Si/Al=32) in 0.2 M solution of sodium hydroxide and tetrabutylammonium hydroxide mixture (TBAOH/(NaOH+TBAOH) = 0.7) at the temperature of 80 °C for 5 h. After desilication, the suspension was cooled down in an ice bath, filtered and washed with distillate water until neutral pH. Next fourfold Na⁺/NH₄⁺ ion-exchange with 0.5 M NH₄NO₃ was performed at 60 °C for 1 h. The resulting material was filtrated, washed and dried at room temperature and finally calcined at 500 °C for 2 h.

B. Characterisation methods

B.1. Elemental analysis

Elemental Si and Al concentrations in the materials were determined by the ICP OES method with an Optima 2100DV (PerkinElmer) spectrometer. The zeolite sample (80-100 mg) was placed in thick walled Teflon digestion vessel and treated with HCl (4 cm³, 35 wt.%) and HF (0.4 cm³, 48 wt.%). The final weight of the solution was adjusted with deionized-distilled water.

B.2. X-Ray diffraction

Wide-angle XRD patterns were obtained with a Rigaku Multiflex diffractometer equipped with Cu K α radiation (40 kV, 40 mA). Powder X-ray patterns were used for the structural identification of all zeolites.

B.3. Nitrogen physisorption

Nitrogen sorption measurements at -196 °C were carried out in a Quantachrome Autosorb-1-MP gas sorption apparatus. Prior to the measurements, all samples were degassed under high vacuum (10-5 mbar) at 400 °C for 16 h. The micropore volume was calculated based on the *t*-plot method. The Brunauer-Emmet-Teller (BET) method was used considering the recommendations of Rouquerol *et al.*^[10] to quantify the apparent specific surface area. The pore size distribution and mesopore volume (*V*_{meso}), in the range between 1.7 and 30 nm) was quantified via the Barrett-Joyner-Halenda (BJH) model on the adsorption branch.^[15]

B.3. Transmission electron microscopy

Transmission electron microscopy (TEM) images were obtained on a Tecnai Osiris microscope (FEI) with a X-FEG Schottky field emitter operated at 200

kV. The materials were dropped onto a holey carbon film supported on a copper grid (Agar Scientific, 300 mesh).

B.4. FTIR and Raman spectroscopy evaluation

Prior to the FTIR study, the material was pressed into the form of self-supporting wafer (ca. 10 mg/cm²) and pre-treated *in-situ* in an on-purpose made IR cell at 500 °C under vacuum conditions (10⁻⁵ bar) for 1 h. The spectra were recorded with resolution of 2 cm⁻¹ in a Bruker Vertex 70 spectrometer equipped with an MCT detector. All the spectra presented in this study were normalized to 10 mg of sample. The sorption of CO (PRAXAIR, 9.5) was performed at -120 °C up to the total saturation of the Lewis acid sites, up to maximum intensities of the 2230-2220 cm⁻¹ and 2190 cm⁻¹ bands, and the appearance of the bands of CO bonded to Brønsted acid sites (2175 cm⁻¹). The total concentrations of Brønsted and Lewis acid sites were determined from quantitative IR studies of pyridine (Py) sorption ($\geq 99.8\%$, Sigma-Aldrich).^[16] The quantitative procedure was based on the Py-gas sorption; the amount sufficient to neutralize all acid sites at 170 °C under static conditions. Subsequently, the gaseous and physisorbed Py molecules were desorbed by vacuum-induced evacuation at the same temperature, which was monitored with the disappearance of the bands related to gas and physisorbed Py. Finally, the band intensities in the latter spectrum were used to calculate the total concentration of Brønsted and Lewis sites, using the intensities (band height) of the 1545 cm⁻¹ band of pyridinium ions (PyH⁺) and the 1450 cm⁻¹ band of Py coordinatively bonded to Lewis sites (PyL). The following absorption coefficients were used: 0.07 cm²· μ mol⁻¹ for the 1545 cm⁻¹ band of pyridinium ion (PyH⁺) and 0.10 cm²· μ mol⁻¹ for the 1450 cm⁻¹ band of pyridine coordinatively bonded to Lewis sites (PyL). The concentrations of the Brønsted and Lewis acid sites accessible for bulky 2,6-di-tert-butylpyridine (di-TBPy, Sigma-Aldrich, $\geq 97\%$), were obtained from experiments where excess of di-TBPy was adsorbed at 200 °C. Subsequently, the physisorbed molecules were desorbed by vacuum-induced evacuation at the same temperature. The sample was then cooled down to room temperature. The band intensities of the di-TBPyH⁺ 1615 cm⁻¹ with absorption coefficient 0.50 cm²· μ mol⁻¹ were employed to quantify the concentration of di-TBPy-accessible acid sites.^[17] The number of carbonaceous species were determined from the relative intensities of the C=C stretching vibrations IR bands associated with conjugated olefins (1660-1585 cm⁻¹) and those associated with disordered aromatic structures (1540-1500 cm⁻¹).

The microRaman analysis was performed with a Renishaw InVia dispersive spectrometer equipped with a CCD detector and integrated with a Leica DMLM confocal microscope. An excitation wavelength of 514.5 nm was provided by an Ar-ion laser (Spectra-Physics, model 2025). The spectra were recorded at ambient conditions with the resolution of 2 cm⁻¹. The Raman scattered light was collected with a 50x Olympus objective in the spectral range of 1000-2000 cm⁻¹. In the Raman spectra the olefinic species were identified by the bands below 1600 cm⁻¹ whereas aromatic moieties were found in the 1700-1600 cm⁻¹ region.

C. Catalytic tests

C.1. Conventional thermogravimetric reactor

The catalytic cracking of low-density polyethylene (LDPE) was evaluated by thermogravimetric analysis in a Perkin-Elmer Pyris 1 analyzer. A stock mixture of the ground polymer and the zeolite powder was prepared in a ratio of polymer : zeolite = 3 : 1; this was prepared by intimately mixing in an Agatha mortar. A certain portion of the mixture (typically 5-10 mg) was loaded in a 70 μ l α -Al₂O₃ crucible and weighted with a 5-digits Mettler Toledo balance before the analysis. The sample was placed in the furnace, the analytic gas was switched on and the temperature was raised from 30 to 600 °C at a heating rate of 5 °C/min under a nitrogen flow of 80 mL/min STP. The conversion was calculated by deducing the catalyst weight and moisture content. Powdery low-density polyethylene was kindly supplied by Sabic Europe.

C.2. Operando reactor

The LDPE catalytic decomposition was studied in operando rig embedded in a flow set-up. The catalyst was mixed with LDPE (1:1) and then assembled in a self-supporting wafers (ca. 5.5-6 mg/cm²) and placed in a home-made 2 cm³ volume IR quartz gas cell. The atmospheric pressure IR reactor cell enables both the analysis of the gas phase through an on-line GC and mass-spectrometer whilst the catalytic surface is simultaneously monitored under the reaction operating conditions. Nitrogen was used as the carrier gas (30 mL/min STP) and introduced through SS 1/16" 110 °C heat-traced pipes. Rapid-scan and time-resolved IR spectra were collected with a Vertex 70 Bruker FT-IR spectrometer, equipped with MCT detectors. The scanner velocity at 80 KHz allows the accumulation of one spectrum (50 scans) per 0.4 min. The spectral resolution was 2 cm⁻¹. The sample wafers in IR cell were heated from room temperature to 180 °C with the rate 2 °C/ sec., then the temperature was rapidly increased to 230 °C with the rate 10 °C/ sec. The amount of the cracking products detected in aforementioned experimental period was negligible, if any, as manifested by the mass spectrometry (Balzers TCP 121) and gas chromatography results (Agilent 7890B, HP-1 column). The specific analysis was carried at 230 °C up to the total LDPE decomposition. The reaction products were analysed simultaneously by a quadrupole mass spectrometer coupled to gas chromatography.

Keywords: waste plastic • cracking • hierarchical zeolites • operando catalysis • ZSM-5

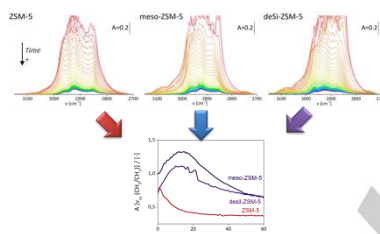
Acknowledgements

The work was financed by the Grant No. 2017/27/B/ST5/00191 from the National Science Centre, Poland. and S.S.Q. thank the European Commission for an Erasmus+ grant.

References

- [1] a) A. Marcilla, A. Gómez-Siurana, F. Valdés, *Journal of Analytical and Applied Pyrolysis* **2007**, *79*, 433-442; b) A. L. Figueiredo, A. S. Araujo, M. Linares, Á. Peral, R. A. García, D. P. Serrano, V. J. Fernandes, *Journal of Analytical and Applied Pyrolysis* **2016**, *117*, 132-140; c) X. Zhang, H. Lei, G. Yadavalli, L. Zhu, Y. Wei, Y. Liu, *Fuel* **2015**, *144*, 33-42.
- [2] a) D. P. Serrano, J. Aguado, J. M. Escola, J. M. Rodríguez, *Journal of Analytical and Applied Pyrolysis* **2005**, *74*, 353-360; b) D. P. Serrano, J. M. Escola, L. Briones, M. Arroyo, *Fuel* **2017**, *206*, 190-198; c) A. Marcilla, M. I. Beltrán, A. Gómez-Siurana, R. Navarro, F. Valdés, *Applied Catalysis A: General* **2007**, *328*, 124-131; d) K. A. Tarach, K. Gora-Marek, J. Martinez-Triguero, I. Melian-Cabrera, *Catalysis Science & Technology* **2017**, *7*, 858-873.
- [3] a) D. P. Serrano, J. Aguado, J. M. Escola, J. M. Rodríguez, L. Morselli, R. Orsi, *Journal of Analytical and Applied Pyrolysis* **2003**, *68-69*, 481-494; b) D. P. Serrano, J. Aguado, J. M. Escola, J. M. Rodríguez, in *Studies in Surface Science and Catalysis, Vol. 142* (Eds.: R. Aiello, G. Giordano, F. Testa), Elsevier, **2002**, pp. 77-84; c) J. F. Mastral, C. Berrueto, M. Gea, J. Ceamanos, *Polymer Degradation and Stability* **2006**, *91*, 3330-3338; d) A. Marcilla, A. Gómez-Siurana, F. J. Valdés, *Applied Catalysis A: General* **2008**, *334*, 20-25; e) A. Marcilla, A. Gómez-Siurana, F. J. Valdés, *Microporous and Mesoporous Materials* **2008**, *109*, 420-428; f) A. Coelho, L. Costa, M. M. Marques, I. M. Fonseca, M. A. N. D. A. Lemos, F. Lemos, *Applied Catalysis A: General* **2012**, *413-414*, 183-191.
- [4] A. Marcilla, A. Gómez-Siurana, F. Valdés, *Polymer Degradation and Stability* **2007**, *92*, 197-204.
- [5] S. Kulprathipanja, *Zeolites in Industrial Separation and Catalysis*, Wiley, **2010**.
- [6] P. Castaño, G. Elordi, M. Olazar, A. T. Aguayo, B. Pawelec, J. Bilbao, *Applied Catalysis B: Environmental* **2011**, *104*, 91-100.
- [7] Y.-H. Seo, K.-H. Lee, D.-H. Shin, *Journal of Analytical and Applied Pyrolysis* **2003**, *70*, 383-398.
- [8] D. W. Park, E. Y. Hwang, J. R. Kim, J. K. Choi, Y. A. Kim, H. C. Woo, *Polymer Degradation and Stability* **1999**, *65*, 193-198.
- [9] a) K. Zhang, M. L. Ostraat, *Catalysis Today* **2016**, *264*, 3-15; b) K. Zhang, S. Fernandez, J. T. O'Brien, T. Pilyugina, S. Kobaslija, M. L. Ostraat, *Catalysis Today* **2018**, *316*, 26-30.
- [10] J. Rouquerol, P. Llewellyn, F. Rouquerol, F. R.-R. J. R. P.L. Llewellyn, N. Seaton, in *Studies in Surface Science and Catalysis, Vol. Volume 160*, Elsevier, **2007**, pp. 49-56.
- [11] J. C. Groen, L. A. A. Peffer, J. Pérez-Ramírez, *Microporous and Mesoporous Materials* **2003**, *60*, 1-17.
- [12] L. M. Kustov, V. B. Kazanskii, S. Beran, L. Kubelkova, P. Jiru, *The Journal of Physical Chemistry* **1987**, *91*, 5247-5251.
- [13] K. A. Tarach, J. Tekla, U. Filek, A. Szymocha, I. Tarach, K. Gora-Marek, *Microporous and Mesoporous Materials* **2017**, *241*, 132-144.
- [14] M. Choi, H. S. Cho, R. Srivastava, C. Venkatesan, D.-H. Choi, R. Ryoo, *Nat Mater* **2006**, *5*, 718-723.
- [15] E. P. Barrett, L. G. Joyner, P. P. Halenda, *Journal of the American Chemical Society* **1951**, *73*, 373-380.
- [16] a) K. Sadowska, K. Gora-Marek, J. Datka, *Vibrational Spectroscopy* **2012**, *63*, 418-425; b) K. Góra-Marek, M. Derewiński, P. Sarv, J. Datka, *Catalysis Today* **2005**, *101*, 131-138.
- [17] K. Gora-Marek, K. Tarach, M. Choi, *Journal of Physical Chemistry C* **2014**, *118*, 12266-12274.

Entry for the Table of Contents



Operando catalysis provides valuable information about how the ZSM-5 catalyst works under reaction conditions for the LDPE cracking. This study illustrates that microporous ZSM-5 gives rise to less cracking and deactivates faster, while hierarchical ZSM-5s are more cracking active with a delayed deactivation, due to the secondary porosity.